Contributions of meteorology and anthropogenic emissions to the trends in winter $PM_{2.5}$ in eastern China 2013−2018

Yanxing Wu[1], Run Liu[1,2*], Yanzi Li[3], Junjie Dong[1], Zhijiong Huang[1,2], Junyu Zheng[1,2] and Shaw Chen Liu[1,2*]

[1]Institute for Environmental and Climate Research, Jinan University, Guangzhou, 511443, China
[2]Guangdong-Hongkong-Macau Joint Laboratory of Collaborative Innovation for Environmental Quality, Guangzhou, 511443, China
[3]Guangzhou Huayue Technology Co., Ltd., Guangzhou, 510630, China

Correspondence to: Run Liu (liurun@jnu.edu.cn), Shaw Chen Liu (shawliu@jnu.edu.cn)

Abstract. Multiple linear regression (MLR) models are used to assess the contributions of meteorology/climate and anthropogenic emission control to linear trends of $PM_{2.5}$ concentration during the period 2013–2018 in three regions in eastern China, namely Beijing-Tianjin-Hebei (BTH), Yangtze River Delta (YRD), and Pearl River Delta (PRD). We find that quantitative contributions to the linear trend of $PM_{2.5}$ derived based on MLR results alone are not credible because a good correlation in the MLR analysis does not imply any causal relationship. As an alternative, we propose that the correlation coefficient should be interpreted as the maximum possible contribution of the independent variable to the dependent variable, and the residual should be interpreted as the minimum contribution of all other independent variables. Under the new interpretation, the previous MLR results become self-consistent. We also find that the results of a short-term (2013–2018) analysis are significantly different from those of a long-term (1985–2018) analysis for the period 2013–2018 they overlap, indicating that MLR results depend critically on the length of time analyzed. The long-term analysis renders a more precise assessment, because of additional constraints provided by the long-term data. We therefore suggest that the best estimates of the contributions of emissions and non-emission processes (including meteorology/climate) to the linear trend in $PM_{2.5}$ during 2013–2018 are those from the long-term analyses: i.e., emission <51% and non-emission >49% for BTH, emission <44% and non-emission >56% for YRD, emission <88% and non-emission >12% for PRD.

1 Introduction

$PM_{2.5}$ (particulate matter with an aerodynamic diameter less than 2.5 μm) pollution has been a severe problem in China that affected human health (Kan et al., 2007; Wang and Mauzerall, 2006; Xu et al., 2013; Cohen et al., 2017), visibility (Han et al., 2014; Zhang et al., 2012; Zhang et al., 2014), the acid deposition problem (Yim et al., 2019; Zhang et al., 2016) as well as the climate systems (Albrecht, 1989; Carslaw et al., 2010; Kok et al., 2018). Recent observations from the China National Environmental Monitoring Center showed a 30%–50% decrease in annual mean $PM_{2.5}$ concentration in China during 2013–2018 (Zhai et al., 2019). These remarkable decreases in the $PM_{2.5}$ concentrations were mostly attributed to emission control of

$PM_{2.5}$ and its precursors in recent studies (e.g., Chen et al., 2019; Gong et al., 2021; Zhai et al., 2019). Using various statistical models, these studies concluded that the control of anthropogenic emissions accounted for 81% to 103% of the reductions of $PM_{2.5}$ in eastern China, suggesting that emissions reductions were crucial to the improvement of air quality in 2013–2018 (Chen et al., 2019; Gong et al., 2021; Zhai et al., 2019). However, Dang and Liao (2019) conducted an investigation with a global 3-D chemical transport model and revealed that transport was the most important process for the occurrence frequency as well as the intensity of severe winter haze days in Beijing–Tianjin–Hebei (BTH) in 2013–2017. Although Dang and Liao (2019) dealt with the severe winter haze rather than the mean haze in BTH, their results suggested that meteorological conditions could exert a critical impact on the reduction in $PM_{2.5}$ in eastern China.

In this study, we use multiple linear regression (MLR) models to investigate the relative contributions of emissions and climate/meteorology processes to linear trends in winter ~~(December-January-February)~~ $PM_{2.5}$ concentration in three major polluted regions in eastern China, namely BTH, Yangtze River Delta (YRD), and Pearl River Delta (PRD). The results can provide important insight for better designing successive clean-air plans to mitigate $PM_{2.5}$ as well as other air pollutants in China. The rest of the paper is structured as follows: The data and methods employed are introduced in Section 2, Section 3 presents the major results and discussions, and Section 4 presents a summary and conclusions.

2 Data and methodology

2.1 Data

Winter visibility data in 1973–2019 are obtained from Global Summary of Day (GSOD) provided by the National Climatic Data Center (NCDC) (https://www.ncei.noaa.gov/maps/daily/, last access: 10 March 2022). The relative humidity (RH) is derived from dew point temperature and air temperature of GSOD following the approach proposed by Lawrence (2005). Surface $PM_{2.5}$ measurements in 2013–2019 are taken from China National Environment Monitoring Center (CNEMC, http://www.cnemc.cn/, last access: 10 March 2022). The $PM_{2.5}$ concentrations were measured by the micro-oscillating balance method and/or the β-absorption method (MEE, 2012; Zhang and Cao, 2015). The autumn (September-October-November) Arctic sea ice index (ASI) is defined as the normalized sea ice fraction north of 45ºN as suggested by Wang et al. (2015), which is calculated from the Hadley Centre (HadISST1: Hadley Centre Sea Ice and Sea Surface Temperature data set, https://www.metoffice.gov.uk/hadobs/hadisst) with 1º×1º resolution for 1870–2022 (Rayner et al., 2003).

PM emission inventories of PM_{10}, $PM_{2.5}$, SO_2, NH_3, NOx, black carbon, and organic carbon in this study are obtained from Peking University (PKU, 1960–2014, 0.1º×0.1º, monthly), which include the fuel consumption and emissions of greenhouse gases and air pollutants from all combustion sources (http://inventory.pku.edu.cn/, last access: 10 November 2021). Multi-resolution Emission Inventory for China (MEIC, version 1.3, 2010–2017, 0.25º×0.25º, monthly, http://www.meicmodel.org, Li et al., 2017; Zheng et al., 2018; last access: 10 November 2021) provided by Tsinghua University, and PRD Emission Inventory (PRD-EI, 2006–2019, 3º×3º, monthly) from Huang et al. (2021) and Zhong et al. (2018) are also used. Due to the

discontinuity of these three inventories, we calculate the scaling factor of each pollutant based on the overlapping period to get a winter inventory from 1985–2018 (Figure 1) in PRD as follows:

$$\text{scaling factor}_{Ei} = \frac{\sum_{2013}^{2006} Ei_{j,PKU}}{\sum_{2013}^{2006} Ei_{j,PRD\text{-}EI}} \quad (1)$$

$$E_i = \begin{cases} Ei_{j,PKU}\ (j=1985, 1986, \ldots 2013) \\ \text{scale factor}_i \times Ei_{j,PRD\text{-}EI}\ (j=2014, 2015, 2016, 2017, 2018) \end{cases} \quad (2)$$

where E_i is emission of species i, the subscripts PKU and PRD-EI denote the PKU inventory and the PRD inventory of Huang et al. (2021) and Zhong et al. (2018), respectively, and j denotes year.

The corresponding formulas for BTH and YRD are:

$$\text{scaling factor}_{Ei} = \frac{\sum_{2013}^{2010} Ei_{j,PKU}}{\sum_{2013}^{2010} Ei_{j,MEIC}} \quad (3)$$

$$E_i = \begin{cases} Ei_{j,PKU}\ (j=1985, 1986, \ldots 2013) \\ \text{scale factor}_i \times Ei_{j,MEIC}\ (j=2014, 2015, 2016) \end{cases} \quad (4)$$

where the subscript MEIC denotes the MEIC inventory.

Since the ratios of annual emission inventories in PRD to those of YRD and BTH are not expected to change significantly in one or two years (Figure S1), the 2016 winter emission ratio of BTH to PRD is multiplied by the 2017 and 2018 winter emission of PRD to obtain the winter emission of BTH in 2017 and 2018. The same is true for 2017 and 2018 winter emission of YRD. The annual emission inventories for BTH, YRD and PRD from 1985 to 2018 are shown in Figure 1. It should be noted that the winter of a specific year in this study includes December of this year and January and February of the following year.

设置了格式: 字体: 10 磅, 英语(美国), 非突出显示

设置了格式: 字体: 10 磅, 英语(美国), 非突出显示

设置了格式: 字体: 10 磅, 英语(美国), 非突出显示

设置了格式: 英语(美国)

2.2 Nonlinear exponential fitting

Since direct observed data of $PM_{2.5}$ are not available before 2013, we employ nonlinear exponential fitting to retrieve $PM_{2.5}$ concentrations in BTH, YRD and PRD from visibility data that have a long-term and complete record. Because RH affects strongly the relationship between $PM_{2.5}$ concentration and visibility (Fu et al., 2016; Liu et al., 2017; L. Zhang et al., 2015; Q. Zhang et al., 2015), we evaluate the relationship for different RH intervals in each region as shown in Figures S2–S4. The r^2 of average fitting is greater than 0.50, some as high as 0.77, significant at 99% confidence level, indicating that the fitting performance is acceptable (Figures S2–S4). As expected, the retrieved $PM_{2.5}$ has a significant negative correlation with visibility (Figure S5). More importantly, the retrieved $PM_{2.5}$ concentrations are in good agreement with the observed $PM_{2.5}$ in recent years from CNEMC (2013–2018) and those observed in US Embassy in Beijing (2009–2018) and Consulates in Shanghai and Guangzhou (2011–2018) (Figure 1). Since the Embassy/Consulates $PM_{2.5}$ data are totally independent of the retrieving of $PM_{2.5}$ concentrations from visibility, the agreement between our retrieved $PM_{2.5}$ concentrations and those observed in US Embassy in Beijing and Consulates in Shanghai and Guangzhou lends strong support for the validity of our retrieved $PM_{2.5}$ concentrations.

A quick inspection of the $PM_{2.5}$ and emission lines in Figure 1 reveals that an expected good regression between $PM_{2.5}$ and emission is only possible for PRD where the emission line matches well with the $PM_{2.5}$ line in general as both have a broad maximum near 2005–2010 (Figure 1c). In BTH a good regression is made difficult due to a critical mismatch characterized by two broad maxima (1985–2000, 2000–2013) in the emission line and a sharp drop after 2013, while the $PM_{2.5}$ line has a shallow depression during the period 1993–2012 followed by a large bulge peaked in 2013 (named hereafter as bulge-2013) and lasted until 2016 (Figure 1a). This mismatch also existed in YRD as the emission line crossed over the $PM_{2.5}$ line in opposite directions near 2012, albeit the bulge was not as large and a depression could be barely seen in 2003–2012 (Figure 1b).

Mao et al. (2019) analyzed extensively the depression 1999–2012 (the deeper part of the 1993–2012 depression) and bulge-2013. They found that the depression and bulge-2013 were primarily caused by a combination of climate oscillations which include negative phases of the Pacific Decadal Oscillation, Arctic Oscillation, El Niño-Southern Oscillation and global temperature, in addition to positive phases of East Asian Winter Monsoon and ASI. It is clear that the presence of bulge-2013 can have a big impact on any study on the contributions of meteorology/climate and anthropogenic emission control to the linear trends in $PM_{2.5}$, especially for a short-term study such as the period 2013–2018 that overlooks the cause of the bulge. This point will be elaborated in Sections 3.3 and 3.4. Finally, given the critical importance of bulge-2013, it is reassuring that the existence of bulge-2013 is independently confirmed by the $PM_{2.5}$ concentrations retrieved from visibility as well as those observed in US Embassy in Beijing and Consulate in Shanghai.

3 Results and discussions

3.1 Multiple linear regression studies

Zhai et al. (2019) constructed a stepwise MLR model to quantify the meteorological contribution to the $PM_{2.5}$ trends. The MLR model made correlation analysis between the 10-day $PM_{2.5}$ anomalies and wind speed, precipitation, RH, temperature, as well as 850 hPa meridional wind velocity. The residual after removing meteorological influence from the MLR model was considered to be driven by changes in anthropogenic emissions. They quantified the contribution of meteorology to $PM_{2.5}$ trends from 2013 to 2018 in BTH, YRD, and PRD at 14%, -3% and 19%, respectively. The residuals, 86%, 103%, and 81% of $PM_{2.5}$ trends were attributed to anthropogenic emissions (Table 1).

Chen et al. (2019) employed Kolmogorov–Zurbenko (KZ) filter to produce an adjusted long-term time series of $PM_{2.5}$ concentrations in Beijing from 2013 to 2017 by removing interannual and seasonal variations in meteorological conditions. They applied MLR models between $PM_{2.5}$ and wind speed, RH, temperature and solar radiation to remove the influence of meteorological conditions and estimated that the contribution of emissions to adjusted $PM_{2.5}$ was 81%, while the contribution of meteorology was 19% (Table 1).

To compare with these two studies, we carry out an MLR analysis on the emission and observed concentrations of $PM_{2.5}$, of which the results will be denoted hereafter as MLR-EMIS. As shown in Figure 2, the observed $PM_{2.5}$ decreased remarkably from 2013 to 2018 in the three regions, with a downward trend of -12.2 $\mu g\ m^{-3}\ yr^{-1}$ in BTH, -7.7 $\mu g\ m^{-3}\ yr^{-1}$ in YRD and -5.0

μg m^{-3} yr^{-1} in PRD. The MLR-EMIS model can mostly capture these decreasing features. The non-emission (residual) in BTH, YRD and PRD has a trend of -0.03 μg m^{-3} yr^{-1}, 0.1 μg m^{-3} yr^{-1} and 0.2 μg m^{-3} yr^{-1} respectively, or 0.2%, -1.0% and -4.0% of the observed trends, respectively. Hence, the contribution of climate/meteorology to the observed linear trend in winter $PM_{2.5}$ in BTH, YRD and PRD from 2013 to 2018 is 0.2%, -1.0% and -4.0% respectively, meaning that 99.8%, 101.0% and 104.0% of the linear trend in the observed winter $PM_{2.5}$ is attributable to emission (Table 1). These results of MLR-EMIS regarding the predominant contribution of emission are in good agreement with Zhai et al. (2019) and Chen et al. (2019). This agreement is reinforced by a mechanistic model assessment conducted by Chen et al. (2019), who suggested that the contribution of emissions to the linear trend in $PM_{2.5}$ in 2013–2017 was 79%, while the contribution by meteorology was only 21%. In addition, Gong et al. (2021) developed a framework based on an Environmental Meteorology Index, to quantitatively assess the contribution of meteorology variations to the trend of $PM_{2.5}$ concentrations and separate the impacts of meteorology from the emission-control measures. They found that emission control contributed more than 90% of the $PM_{2.5}$ trend in BTH from 2013 to 2017, again in good agreement with those values in BTH and Beijing shown in Table 1 (upper two rows).

Wang et al. (2015) hypothesized that the decreasing ASI could be an important contributor to the recent increase in haze days in eastern China, and about 45–67% of the interannual to interdecadal variability of winter haze days could be explained by the ASI variability. Following the MLR-EMIS model study above, we carry out a parallel MLR-ASI model study in which the emission is replaced by ASI (Figure 3). The non-ASI trends (residuals) contribute -9.3 μg m^{-3} yr^{-1}, -3.3 μg m^{-3} yr^{-1} and -3.0 μg m^{-3} yr^{-1}, respectively, to the observed linear trends in winter $PM_{2.5}$ in BTH, YRD and PRD, which imply that the emissions (non-ASI) are responsible for 76%, 43% and 60% of the observed linear trend in winter $PM_{2.5}$ in BTH, YRD and PRD, respectively, in 2013–2018 (Table 2). It follows that ASI can explain 24%, 57% and 40% of the decreasing trends in BTH, YRD and PRD, respectively (Table 2), which are on the low side but nevertheless in qualitative agreement with Wang et al. (2015). Here we note that the contribution of ASI represents only a partial contribution of climate/meteorological conditions, adding other meteorological parameters would increase the contribution.

The comparison of Tables 1 and 2 poses an interesting problem. For BTH, the MLR-ASI value of 76% (Table 2) for the contribution of emissions is slightly lower than, but nevertheless agrees qualitatively with the results of MLR-EMIS in the upper two rows of Table 1. However, for YRD and PRD, the contributions of 43% and 60% (Table 2), respectively, by non-ASI (including emissions) to the observed linear trends in winter $PM_{2.5}$ are significantly less than those values of 101%–104% derived by the MLR-EMIS analysis (bottom two rows of Table 1). What causes the discrepancy? Which table has the correct results? The answer to the first question is that there were significant linear trends in $PM_{2.5}$, anthropogenic emissions and ASI in 2013-2018 (Figures 1 and 3), but there was no significant linear trend in 2013-2018 in the meteorological parameters used in the studies by Zhai et al. (2019) and Chen et al. (2019). The MLR analysis gives high values to correlation coefficients of parameters with significant linear trends. In fact, any parameter with a significant linear trend in 2013–2018, e.g., sea surface temperature (SST) of the western Pacific, would get a high correlation coefficient in the MLR analysis.

3.2 Comparing the MLR results to mechanistic models

The answer to the question whether Table 1 or 2 is correct is that neither of them is correct, for the following reasons: All evaluations in Tables 1 and 2 quantified the contributions of anthropogenic emission and meteorology to the linear trend of $PM_{2.5}$ in 2013−2018 using certain statistical MLR models. No mechanistic process was considered in these models. This raises a fundamental concern about the attribution of causes based on statistical regression results alone. It is well known that a good correlation in the MLR analysis does not imply any causal relationship. The causal relationship can only be established if a mechanistic model, that simulates the atmospheric environment with realistic emissions of air pollutants and ambient meteorological conditions as model inputs, can credibly reproduce the observed concentrations and trends of $PM_{2.5}$. Therefore, we conclude that the quantitative results in Tables 1 and 2 are not scientifically credible unless corroborated by a mechanistic model.

The KZ-MLR results of Chen et al. (2019) in Table 1 were corroborated by the Weather Research and Forecasting and the Community Multi-scale Air Quality model (WRF-CMAQ), a mechanistic model (Chen et al., 2019). However, the mechanistic model study of Chen et al., (2019) was consisted of short term (2013–2017) simulations. As noted in Section 2.2, a short-term study of 2013–2017 overlooks the effect and the cause of bulge-2013, which might lead to significant uncertainties and/or biased results. In this context, we believe that a credible mechanistic (or MLR) model study should cover long enough time before the period of interest (2013–2018), so that the model could be constrained by the major features of interannual variations such as bulge-2013 and the depression before it (Figure 1a).

We summarize the discussions involving Tables 1 and 2 as follows. (1) Quantitative MLR results in Tables 1 and 2 without corroboration by a mechanistic model are not credible. (2) Results from mechanistic models are more credible than MLR in theory, but significant uncertainties and/or biased results exist in the short-term model simulations.

3.3 An alternative interpretation of MLR results

In view of the difficulty in interpreting the results from MLR analysis, we propose an alternative interpretation of the correlation coefficient by interpreting it as “the maximum possible contribution of an independent variable (e.g., emissions in Table 1) to the dependent variable (e.g., linear trends of $PM_{2.5}$ in Table 1)”, while the residual should be interpreted as the minimum contribution of all other independent variables (e.g., non-emission variables such as meteorological parameters in Table 1). A theoretical foundation in support of this alternative interpretation can be understood as follows: The MLR analysis is, in effect, performing an optimum-fit between the independent variable and the dependent variable. In other words, the optimum-fit enables the independent variable (e.g., emission in our case) to attain the optimum/maximized contribution to the variability (including the linear trend) of the dependent variable (e.g., $PM_{2.5}$). Furthermore, the “the maximum possible contribution” in the alternative interpretation is reinforced because all-factors-other-than-emission (e.g., ASI) that may contribute to the variability (including the linear trend) are excluded in the optimum-fit process.

Tables 3 and 4 are the corresponding outcomes from the new interpretation for Tables 1 and 2, respectively. It is clear that under the new interpretation, Tables 3 and 4, unlike Tables 1 and 2, are now consistent with each other. In addition, the results of Chen et al. (2019) and Gong et al. (2021), under the new interpretation, are also consistent with the range of values in Tables 3 and 4. These consistent results provide a solid cornerstone to explore additional applications of the alternative interpretation as discussed in Section 3.4.

Another critical factor affecting the MLR results is the length of time period studied. Table 5 compares the results of two short-term studies (2013–2017; 2013–2018) in BTH to a long-term study (1985–2018) for MLR-EMIS and MLR-ASI. The emissions of MLR-EMIS can contribute to a maximum of 101% of the observed trend of $PM_{2.5}$ in BTH during 2013–2017, while the residual parameters contribute at least -1%. For the MLR-ASI analysis, the maximum possible contribution of ASI to observed $PM_{2.5}$ in 2013–2017 is 30%, while the residuals (including emissions) contribute at least 70%. Using the retrieved $PM_{2.5}$ does not change the results significantly from the observed $PM_{2.5}$. Adding 2018 into consideration makes little difference for MLR-EMIS. However, adding only the year 2018, the ASI's maximum possible contribution to observed $PM_{2.5}$ declines by about 11% compared to that of 2013–2017, while the minimum contribution of the residual increases from 57% to 68% (Table 5). The reason for the larger change in the MLR-ASI can be readily understood by comparing the solid red line (EMIS) in Figure 2a to that (ASI) of Figure 3a, the former maintained a smooth declining trend in 2016–2018 while the latter turned around and increased from 2016 to 2018. This turning-around made the MLR-ASI regression significantly worse and was responsible for the residual increasing from 57% to 68%.

The 2013–2017 and 2013–2018 results of MLR-EMIS in YRD (Table 6) and PRD (Table 7) were also consistent with those in BTH (Table 5). The 2013–2017 and 2013–2018 results of MLR-ASI in PRD were consistent with those in BTH, while the values of corresponding results of YRD were relatively large compared with the other two regions. The reason for the difference was that the solid red line (ASI) and the solid black line (observed $PM_{2.5}$) in YRD showed relatively consistent trends from 2013 to 2017, while both lines showed opposite trends in the 2014–2017 BTH and 2015–2018 PRD (Figure 3). The consistent trend between the two lines made the MLR-ASI regression in YRD relatively good, resulting in the maximum contribution of ASI to $PM_{2.5}$ in YRD from 2013 to 2017 being 80%, while the residual contribution was greater than 20%. After adding the opposite upward trend of the two curves from 2017 to 2018, the maximum ASI contribution to $PM_{2.5}$ in YRD decreased substantially from 85% to 54%, while the residual increased to >46% (Table 6).

Extending to 1985–2018, these long-term results differed drastically from the short-term results: The contribution of emissions in MLR-EMIS to the linear trends of $PM_{2.5}$ in BTH for the 34-year study was merely <7%, while the contribution of all residual parameters was >93%. The small upper limit of 7% can be easily explained by examining Figure 4a in which the regression between the red line (emission) and black line ($PM_{2.5}$) is very poor, especially after 2010 when the observed $PM_{2.5}$ started to climb from around 20% to the bulge-2013 of 100%. In fact, the red emission line in Figure 1a had to be turned upside down in Figure 4a to get the best fit to the black line of $PM_{2.5}$ (note the fit between 1988 and 2012 was fairly good), which resulted in the red line to miss the bulge-2013 completely. The small contribution of emissions compared to the residuals is in good agreement with the mechanistic model results of Dang and Liao (2019) who found that meteorology contributed significantly

more than emissions to the linear trend as well as the interannual variability of severe winter haze days in BTH in 2013−2017. The MLR-ASI analysis for $PM_{2.5}$ in BTH over the 34-year period from 1985 to 2018 had a slightly better regression result as shown in Figure 5a. As a result, the maximum possible contribution of ASI to the linear trend of $PM_{2.5}$ was 43%, while the minimum contribution of the residuals was 57% (Table 5). The bulge-2013 in the winter haze days in North China Plain was also noticed by Yin and Wang (2017), whose generalized additive model using ASI and SST as predictors was found to capture the interannual and interdecadal variations of winter haze days in 1980−2015, including the bulge-2013.

For YRD, the 1985–2018 emission contribution to the linear trend in the observed $PM_{2.5}$ had an upper limit of only 1%, implying the contribution of residuals (including meteorology) to be at least 99% (Table 6). The small 1% can be explained by the extremely poor match between the red line (emission) and the black line ($PM_{2.5}$) in Figure 4b. The regression result of the MLR-ASI analysis in YRD was relatively good. Although the red line (ASI) also failed to match bulge-2013, it matched well with the 2016−2018 profile as shown in Figure 5b. As a result, the maximum possible contribution of ASI to the 34-year linear trend of $PM_{2.5}$ reached 75%, implying the minimum contribution of the residuals to be 25% (Table 6). PRD did not have the bulge-2013 (Figure 1c) and therefore had a good regression between emissions and $PM_{2.5}$ from 1985 to 2018 (Figure 4c), implying that emissions over 34-year period could contribute as much as 157% to the linear trend of $PM_{2.5}$, while >-57% was contributed by the residuals (Table 7). The regression result of the MLR-ASI analysis for $PM_{2.5}$ in PRD from 1985 to 2018 was slightly better than those of the MLR-EMIS, and the red line (ASI) and the black line ($PM_{2.5}$) showed opposite trends only in 2011−2015 as shown in Figure 5c, resulting in the maximum contribution of ASI to the linear trend of $PM_{2.5}$ being 81%, while the minimum contribution of the residuals was 19% (Table 7).

3.4 Best estimate of the contribution

Tables 5−7 and Figures 4−5 provide strong evidence supporting the notion that the contributions of emissions and meteorology to the linear trend in $PM_{2.5}$ depend on the length of time analyzed. A critical question remaining is which regression analysis gives the correct value of the contribution when a long-term analysis overlaps with a short-term analysis, e.g., the $1985{-}2018^{ret}$ analysis (Figure 4a) vs. the $2013{-}2018^{ret}$ analysis (Figure 2a) for BTH during the period 2013−2018 (fourth row vs. last row in Table 5)? A logical answer to this question is that the long-term analysis gives the correct value because it has more data points to constrain the regression. This is discussed in the following using the BTH case as an example.

Figure 4a-a shows an enlarged plot of the 2013−2018 portion of Figure 4a (named as $2013{-}2018^{ret34}$ analysis hereafter and in Tables 5−7). The green solid bars in Figure 4a-a denote the anomalies/deviations of the red emission line from the black observations line, of which the mean absolute value of 49% (third column and the last row of Table 5) can be recognized as the minimum contribution of the residual/non-emission (including meteorology/climate) to the linear trend in $PM_{2.5}$ according to the alternative interpretation. Hence the maximum possible contribution by EMIS is 51%, which is substantially less than the 94% of the $2013{-}2018^{ret}$ analysis (second column and fourth row of Table 5). The main reason for this difference can be traced to the bulge-2013 in Figure 4a which, as discussed in Section 3.3, contributes pivotally to the red emission line in Figure 1a being turned upside down in Figure 4a to get the best fit with the black line of observed $PM_{2.5}$. For the $2013{-}2018^{ret34}$ ASI

analysis, the green solid bars of Figure 5a-a denote the anomalies/deviations of ASI line from the $PM_{2.5}$ line, of which the mean absolute value of 38% (fifth column and last row of Table 5) can be recognized as the minimum contribution of the residual of ASI, which includes emissions. Hence, we derive the maximum possible contribution by ASI to be 62% (fourth column and last row of Table 5). Key results of the two analyses above are summarized in the fourth and last rows of Table 5. Qualitatively the results of the $2013-2018^{ret}$ analysis and the $2013-2018^{ret34}$ analysis are consistent (overlap) with each other, quantitatively a significant difference exists between the two analyses: the contribution of emission to the linear trend in $PM_{2.5}$ in the latter has a tighter upper limit of only 51% compared to 94% of the former, and a greater lower limit for the contribution of the residual which includes meteorology/climate in the latter (49%) compared to the former (6%). The fact that the long-term analysis renders a tighter upper/lower limit is evidently the result of additional constraints provided by the long-term data. Finally, since a tighter upper/lower limit gives a more precise estimate of the contribution, we propose that the best estimates of the contributions of emission, ASI and other meteorology/climate parameters to the linear trend in $PM_{2.5}$ in BTH during 2013−2018 are those listed in the last row of Table 5, specifically, emission<51%, non-emission>49%, ASI<62% and non-ASI>38%. These are our best estimates which are remarkably different from those of MLR studies listed in Table 1.

The same analysis can be carried out for YRD and PRD, and the key results are summarized in the fourth and last rows of Tables 6 and 7, respectively. For YRD, the best estimates of the contributions of emission, ASI and other meteorology/climate parameters to the linear trend in $PM_{2.5}$ during 2013−2018 are those listed in the last row of Table 6, specifically, emission<44%, non-emission>56%, ASI<74% and non-ASI>26%. For PRD, the best estimates of the contributions of emission, ASI and other meteorology/climate parameters to the linear trend in $PM_{2.5}$ during 2013−2018 are those listed in the last row of Table 7, specifically, emission<88%, non-emission>12%, ASI<55% and non-ASI>45%. These best estimates are also significantly different from those of MLR studies listed in Table 1.

4 Summary and conclusions

Recently, Chen et al. (2019) and Zhai et al. (2019) used MLR models to analyze the significant downward trend of $PM_{2.5}$ concentrations in China's major air pollution regions in 2013–2018 (2013–2017 for Chen et al. (2019)) and quantified that the control of anthropogenic emissions accounted for 81% to 103% of the $PM_{2.5}$ reduction (Table 1). While there is little doubt that anthropogenic emissions make a significant contribution to the reduction trend of $PM_{2.5}$, we are skeptical of these high contributions by emissions obtained based solely on MLR models, because a good correlation in MLR analysis does not imply any causal relationship. In this regard, Chen et al. (2019) corroborated their MLR result of 81% (Table 1) using the mechanistic model WRF-CMAQ. However, the mechanistic model study of Chen et al., (2019) was consisted of short term (2013–2017) simulations. As noted in Section 2.2, a short-term study of 2013–2017 overlooked the effect and the cause of bulge-2013, which could lead to significant uncertainties and/or biased results. In this context, we believe that a credible mechanistic (or MLR) model study should cover long enough time before the period of interest (2013–2017), so that the model could be constrained by the major features of interannual variations such as the bulge-2013 and the depression before it (Figure 1a).

To compare with previous MLR studies, the MLR model is used in this study to assess the contributions of climate/meteorology and anthropogenic emissions to the linear trends of $PM_{2.5}$ concentration in three regions in eastern China, namely BTH, YRD, and PRD. We first carry out an MLR analysis (MLR-EMIS) on the emissions and observed trend of $PM_{2.5}$ in BTH during 2013−2018, and show that the results of Zhai et al. (2019) and Chen et al. (2019) can be satisfactorily reproduced (Table 1). Then the same MLR analysis are performed on ASI and observed trend of $PM_{2.5}$ (MLR-ASI), and obtain a 76% contribution by emissions in BTH, which is slightly lower than, but nonetheless in qualitative agreement with those values obtained by Zhai et al. (2019) and Chen et al. (2019) (Tables 1 and 2). However, for YRD and PRD, the contributions of emissions to the observed trends of $PM_{2.5}$ are only 43% and 60% (Table 2), respectively, significantly less than those values of 101%−104% derived by the MLR-EMIS analysis (Table 1). We believe that the discrepancy is rooted in the false assumption/interpretation of the correlation coefficient as the value of contribution in the MRL studies as discussed earlier. We therefore propose an alternative interpretation: the correlation coefficient should be interpreted as the maximum possible contribution of the independent variable to the dependent variable, and the residual should be interpreted as the minimum contribution of all other independent variables. Under the new interpretation, all ~~the new~~previous results~~,~~ as shown in Tables 3–4, become consistent with one another.

Another important outcome from this study is that the results of a short-term (2013–2018) analysis are significantly different from those of a long-term (1985–2018) analysis for the period 2013−2018 they overlap, suggesting that MLR results depend critically on the length of time analyzed. The long-term analysis renders a more precise estimate, because of additional constraints provided by the long-term data. We therefore suggest that the best estimates of the contributions of emissions and non-emission (including climate/meteorology) to the linear trend in $PM_{2.5}$ during 2013–2018 are those from the long-term analyses: i.e., emission <51% and non-emission >49% for BTH, emission <44% and non-emission >56% for YRD, emission <88% and non-emission >12% for PRD.

Data availability. Visibility data were obtained from Global Summary of Day (GSOD) provided by the National Climatic Data Center (NCDC) (https://www.ncei.noaa.gov/maps/daily/, last access: 10 March 2022). Surface $PM_{2.5}$ measurements from 2013–2019 are taken from China National Environment Monitoring Center (CNEMC, http://www.cnemc.cn/, last access: 10 March 2022). The data of this paper are available upon request to Shaw Chen Liu (shawliu@jnu.edu.cn).

Author Contributions. RL and SL proposed the essential research idea. YW performed the analysis. YW, RL and SL drafted the manuscript. JD, YL, ZH and JZ helped analysis and offered valuable comments. All authors have read and agreed to the published version of the manuscript.

Competing interests. The authors declare that they have no conflict of interest.

Acknowledgments. The authors thank National Climatic Data Center (NCDC) and the China National Environmental Centre for providing datasets that made this work possible. We also acknowledge the support of the Institute for Environmental and Climate Research and Guangdong-Hong Kong-Macau Joint Laboratory of Collaborative Innovation for Environmental Quality in Jinan University.

Financial support. This work was jointly supported by the National Natural Science Foundation of China (92044302, 41805115), Guangzhou Municipal Science and Technology Project, China (202002020065), Special Fund Project for Science and Technology Innovation Strategy of Guangdong Province (2019B121205004), and Guangdong Innovative and Entrepreneurial Research Team Program (2016ZT06N263).

References

Albrecht B. A.: Aerosols, cloud microphysics, and fractional cloudiness, Science, 245(4923), 1227–1230, https://doi.org/10.1126/science.245.4923.1227, 1989.

Cohen, A. J., Brauer, M., Burnett, R., Anderson, H. R., Frostad, J., Estep, K., Balakrishnan, K., Brunekreef, B., Dandona, L. and Dandona, R.: Estimates and 25-year trends of the global burden of disease attributable to ambient air pollution: an analysis of data from the Global Burden of Diseases Study 2015, The Lancet, 389, 1907–1918, https://doi.org/10.1016/S0140-6736(17)30505-6, 2017.

Carslaw, K. S., Boucher, O., Spracklen, D. V., Mann, G. W., Rae, J. G. L., Woodward, S. and Kulmala, M.: A review of natural aerosol interactions and feedbacks within the Earth system, Atmos. Chem. Phys., 10(4), 1701–1737, https://doi.org/10.5194/acp-10-1701-2010, 2010.

Chen, Z., Chen, D., Kwan, M. P., Chen, B., Gao, B., Zhuang, Y., Li, R. and Xu, B.: The control of anthropogenic emissions contributed to 80% of the decrease in $PM_{2.5}$ concentrations in Beijing from 2013 to 2017, Atmos. Chem. Phys., 19(21), 13519–13533, https://doi.org/10.5194/acp-19-13519-2019, 2019.

Dang, R. and Liao, H.: Severe winter haze days in the Beijing-Tianjin-Hebei region from 1985 to 2017 and the roles of anthropogenic emissions and meteorology, Atmos. Chem. Phys., 19(16), 10801–10816, https://doi.org/10.5194/acp-19-10801-2019, 2019.

Fu, X., Wang, X., Hu, Q., Li, G., Ding, X., Zhang, Y., He, Q., Liu, T., Zhang, Z., Yu, Q., Shen, R. and Bi, X.: Changes in visibility with $PM_{2.5}$ composition and relative humidity at a background site in the Pearl River Delta region, J. Environ. Sci., 40, 10–19, https://doi.org/10.1016/j.jes.2015.12.001, 2016.

Gong, S., Liu, H., Zhang, B., He, J., Zhang, H., Wang, Y., Wang, S., Zhang, L. and Wang, J.: Assessment of meteorology vs. control measures in the China fine particular matter trend from 2013 to 2019 by an environmental meteorology index, Atmos. Chem. Phys., 21(4), 2999–3013, https://doi.org/10.5194/acp-21-2999-2021, 2021.

Han, X., Zhang, M., Gao, J., Wang, S. and Chai, F.: Modeling analysis of the seasonal characteristics of haze formation in Beijing, Atmos. Chem. Phys., 14(18), 10231–10248, https://doi.org/10.5194/acp-14-10231-2014, 2014.

Huang, Z., Zhong, Z., Sha, Q., Xu, Y., Zhang, Z., Wu, L., Wang, Y., Zhang, L., Cui, X., Tang, M. S., Shi, B., Zheng, C., Li, Z., Hu, M., Bi, L., Zheng, J. and Yan, M.: An updated model-ready emission inventory for Guangdong Province by incorporating big data and mapping onto multiple chemical mechanisms, Sci. Total Environ., 769, 144535, https://doi.org/10.1016/j.scitotenv.2020.144535, 2021.

Kan, H., London, S. J., Chen, G., Zhang, Y., Song, G., Zhao, N., Jiang, L. and Chen, B.: Differentiating the effects of fine and coarse particles on daily mortality in Shanghai, China, Environ. Int., 33(3), 376–384, https://doi.org/10.1016/j.envint.2006.12.001, 2007.

Kok, J. F., Ward, D. S., Mahowald, N. M. and Evan, A. T.: Global and regional importance of the direct dust-climate feedback, Nat. Commun., 9(1), 1–11, https://doi.org/10.1038/s41467-017-02620-y, 2018.

Lawrence, M. G.: The relationship between relative humidity and the dewpoint temperature in moist air: A simple conversion and applications, Bull. Am. Meteorol. Soc., 86(2), 225–233, https://doi.org/10.1175/BAMS-86-2-225, 2005.

Li, M., Liu, H., Geng, G., Hong, C., Liu, F., Song, Y., Tong, D., Zheng, B., Cui, H., Man, H., Zhang, Q. and He, K.: Anthropogenic emission inventories in China: A review, Natl. Sci. Rev., 4, 834–866, https://doi.org/10.1093/nsr/nwx150, 2017.

Liu, M., Bi, J. and Ma, Z.: Visibility-based $PM_{2.5}$ concentrations in China: 1957–1964 and 1973–2014, Environ. Sci. Technol., 51(22), 13161–13169, https://doi.org/10.1021/acs.est.7b03468, 2017.

Mao, L., Liu, R., Liao, W., Wang, X., Shao, M., Liu, S. C. and Zhang, Y.: An observation-based perspective of winter haze days in four major polluted regions of China, Natl. Sci. Rev., 6(3), 515–523, https://doi.org/10.1093/nsr/nwy118, 2019.

MEE (Ministry of Ecology and Environment of the People's Republic of China): Ambient Air Quality Standards, GB 3095–2012, 2012.

Rayner, N. A., Parker, D. E., Horton, E. B., Folland, C. K., Alexander, L. V., Rowell, D. P., Kent, E. C. and Kaplan, A.: Global analyses of sea surface temperature, sea ice, and night marine air temperature since the late nineteenth century, J. Geophys. Res. Atmos., 108(14), https://10.1029/2002jd002670, 2003.

Wang, H. J., Chen, H. P., and Liu, J.: Arctic Sea ice decline intensified haze pollution in Eastern China, Atmos. Oceanic. Sci. Lett., 8(1), 1–9, https://doi.org/10.3878/AOSL20140081, 2015.

Wang, X. and Mauzerall, D. L.: Evaluating impacts of air pollution in China on public health: Implications for future air pollution and energy policies, Atmos. Environ., 40(9), 1706–1721, https://doi.org/10.1016/j.atmosenv.2005.10.066, 2006.

Xu, P., Chen, Y. and Ye, X.: Haze, air pollution, and health in China, The Lancet, 382(9910), 2067, https://doi.org/10.1016/S0140-6736(13)62693-8, 2013.

Yin, Z. and Wang, H.: Statistical prediction of winter haze days in the North China plain using the generalized additive model, J. Appl. Meteorol. Climatol., 56(9), 2411–2419, https://doi.org/10.1175/JAMC-D-17-0013.1, 2017.

Yim, S. H. L., Gu, Y., Shapiro, M. and Stephens, B.: Air quality and acid deposition impacts of local emissions and transboundary air pollution in Japan and South Korea, Atmos. Chem. Phys., 19, 13309–13323, https://doi.org/10.5194/acp-19-13309-2019, 2019.

Zhai, S., Jacob, D. J., Wang, X., Shen, L., Li, K., Zhang, Y., Gui, K., Zhao, T. and Liao, H.: Fine particulate matter ($PM_{2.5}$) trends in China, 2013–2018: Separating contributions from anthropogenic emissions and meteorology, Atmos. Chem. Phys., 19(16), 11031–11041, https://doi.org/10.5194/acp-19-11031–2019, 2019.

Zhang, R. H., Li, Q. and Zhang, R. N.: Meteorological conditions for the persistent severe fog and haze event over eastern China in January 2013, Sci. China Earth Sci., 57(1), 26–35, https://doi.org/10.1007/s11430-013-4774-3, 2014.

Zhang, X. Y., Wang, Y. Q., Niu, T., Zhang, X. C., Gong, S. L., Zhang, Y. M. and Sun, J. Y.: Atmospheric aerosol compositions in China: Spatial/temporal variability, chemical signature, regional haze distribution and comparisons with global aerosols, Atmos. Chem. Phys., 12(2), 779–799, https://doi.org/10.5194/acp-12-779-2012, 2012.

Zhang, Y. L. and Cao, F.: Fine particulate matter ($PM_{2.5}$) in China at a city level, Sci. Rep., 5, 14884, https://doi.org/10.1038/srep14884, 2015.

Zhang, Y., Huang, W., Cai, T., Fang, D., Wang, Y., Song, J., Hu, M. and Zhang, Y.: Concentrations and chemical compositions of fine particles ($PM_{2.5}$) during haze and non-haze days in Beijing, Atmos. Res., 174–175, 62–69, https://doi.org/10.1016/j.atmosres.2016.02.003, 2016.

Zhang, L., Sun, J. Y., Shen, X. J., Zhang, Y. M., Che, H., Ma, Q. L., Zhang, Y. W., Zhang, X. Y. and Ogren, J. A.: Observations of relative humidity effects on aerosol light scattering in the Yangtze River Delta of China, Atmos. Chem. Phys., 15(14), 8439–8454, https://doi.org/10.5194/acp-15-8439-2015, 2015.

Zhang, Q., Quan, J., Tie, X., Li, X., Liu, Q., Gao, Y. and Zhao, D.: Effects of meteorology and secondary particle formation on visibility during heavy haze events in Beijing, China, Sci. Total Environ., 502, 578–584, https://doi.org/10.1016/j.scitotenv.2014.09.079, 2015.

Zheng, B., Tong, D., Li, M., Liu, F., Hong, C., Geng, G., Li, H., Li, X., Peng, L., Qi, J., Yan, L., Zhang, Y., Zhao, H., Zheng, Y., He, K. and Zhang, Q.: Trends in China's anthropogenic emissions since 2010 as the consequence of clean air actions, Atmos. Chem. Phys., 18, 14095–14111, https://doi.org/10.5194/acp-18-14095-2018, 2018.

Zhong, Z., Zheng, J., Zhu, M., Huang, Z., Zhang, Z., Jia, G., Wang, X., Bian, Y., Wang, Y. and Li, N.: Recent developments of anthropogenic air pollutant emission inventories in Guangdong province, China, Sci. Total Environ., 627, 1080–1092, https://doi.org/10.1016/j.scitotenv.2018.01.268, 2018.

Table 1: Comparison of the contribution of emissions and meteorological conditions to the observed $PM_{2.5}$ trends in 2013−2018 (2013−2017 for Chen et al. (2019)).

Research	Region	Method	Emission	Meteorology
Chen et al. (2019)	Beijing	KZ-MLR	81%	19%
Zhai et al. (2019)	BTH	MLR	86%	14%
This study		MLR-EMIS	99.8%	0.2%
Zhai et al. (2019)	YRD	MLR	103%	-3%
This study		MLR-EMIS	101%	-1%
Zhai et al. (2019)	PRD	MLR	81%	19%
This study		MLR-EMIS	104%	-4%

Note: KZ: Kolmogorov–Zurbenko filter; MLR: stepwise multiple linear regression; MLR-EMIS indicates the use of emissions and $PM_{2.5}$ as inputs to the MLR model.

Table 2: Contributions of arctic sea ice (ASI) and residuals (Non-ASI) to the observed $PM_{2.5}$ trends in the winter seasons of 2013−2018.

Region	Method	ASI	Non-ASI
BTH		24%	76%
YRD	MLR-ASI	57%	43%
PRD		40%	60%

Note: MLR-ASI indicates the use of ASI and $PM_{2.5}$ as inputs to the MLR model.

Table 3. Contributions of emissions and non-emissions (including climate and meteorological conditions) to the observed $PM_{2.5}$ trends in 2013−2018 (2013−2017 for Chen et al. (2019)).

Research	Region	Method	Emission	Non-emission
Chen et al. (2019)	Beijing	KZ-MLR	<81%	>19%
Zhai et al. (2019)	BTH	MLR	<86%	>14%
This study		MLR-EMIS	<99.8%	>0.2%
Zhai et al. (2019)	YRD	MLR	<103%	>-3%
This study		MLR-EMIS	<101%	>-1%
Zhai et al. (2019)	PRD	MLR	<81%	>19%
This study		MLR-EMIS	<104%	>-4%

Table 4. Contributions of ASI and residuals (Non-ASI) to the observed $PM_{2.5}$ trends in 2013−2018.

Region	Method	ASI	Non-ASI
BTH		<24%	>76%
YRD	MLR-ASI	<57%	>43%
PRD		<40%	>60%

Table 5. Contributions of emissions and ASI to the $PM_{2.5}$ trends in BTH.

Time Period	MLR-EMIS		MLR-ASI	
	Emission	Non-emission	ASI	Non-ASI
$2013-2017^{obs}$	<101%	>-1%	<30%	>70%
$2013-2017^{ret}$	<94%	>6%	<43%	>57%
$2013-2018^{obs}$	<99.8%	>0.2%	<24%	>76%
$2013-2018^{ret}$	<94%	>6%	<32%	>68%
$1985-2018^{ret}$	<7%	>93%	<43%	>57%
$2013-2018^{ret34}$	<51%	>49%	<62%	>38%

Note: The superscripts obs and ret indicate the use of observed and retrieved $PM_{2.5}$ data, respectively. Superscript ret34 indicates the retrieved $PM_{2.5}$ data for 2013–2018 obtained using the data of 1985–2018.

Table 6. Contributions of emissions and ASI to the $PM_{2.5}$ trends in YRD.

Time Period	MLR-EMIS		MLR-ASI	
	Emission	Non-emission	ASI	Non-ASI
2013−2017[obs]	<104%	>-4%	<80%	>20%
2013−2017[ret]	<84%	>16%	<85%	>15%
2013−2018[obs]	<101%	>-1%	<57%	>43%
2013−2018[ret]	<86%	>14%	<54%	>46%
1985−2018[ret]	<1%	>99%	<75%	>25%
2013−2018 [ret34]	<44%	>56%	<74%	>26%

Table 7. Contributions of emissions and ASI to the $PM_{2.5}$ trends in PRD.

Time Period	MLR-EMIS		MLR-ASI	
	Emission	Non-emission	ASI	Non-ASI
2013−2017[obs]	<119%	>-19%	<67%	>33%
2013−2017[ret]	<104%	>-4%	<59%	>41%
2013−2018[obs]	<104%	>-4%	<40%	>60%
2013−2018[ret]	<99.5%	>0.5%	<39%	>61%
1985−2018[ret]	<157%	>-57%	<81%	>19%
2013−2018 [ret34]	<88%	>12%	<55%	>45%

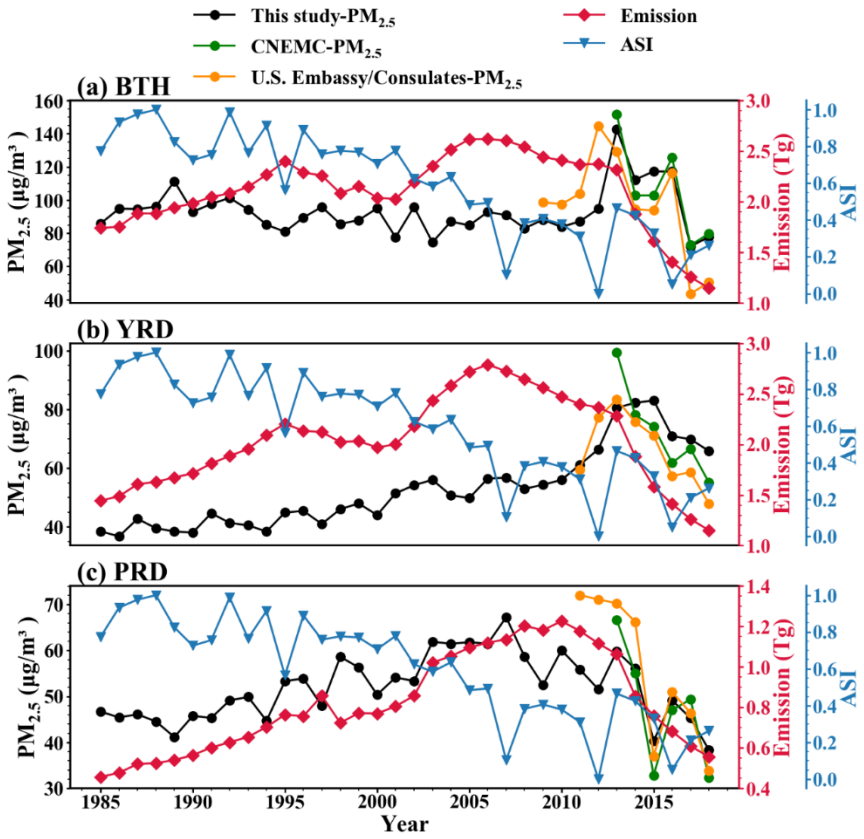

Figure 1: Annual winter averages of retrieved $PM_{2.5}$ concentrations (black, 1985–2018), emission (red, 1985–2018), Arctic Sea Ice (ASI, blue, 1985–2018) in BTH, YRD and PRD; $PM_{2.5}$ concentrations observed by the US Embassy/Consulates in Beijing (orange, 2009–2018), Shanghai and Guangzhou (orange, 2011–2018); and $PM_{2.5}$ concentrations observed by CNEMC (green, 2013–2018).

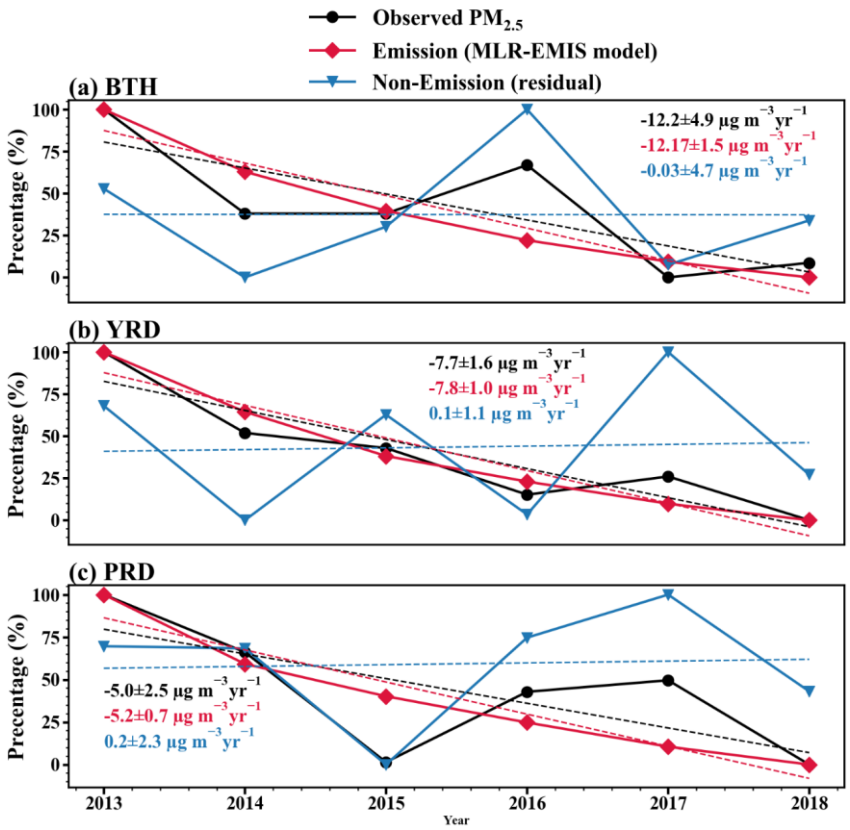

435

Figure 2: Results of MLR-EMIS analysis for 2013–2018 in BTH (a), YRD (b) and PRD (c). Temporal variations of observed winter $PM_{2.5}$ concentration are shown in black, contributions of anthropogenic emissions to the $PM_{2.5}$ trend are shown in red, and the residual is shown in blue. Values inset in each panel are the ordinary linear regression trends, with 95% confidence intervals obtained by the student's t test.

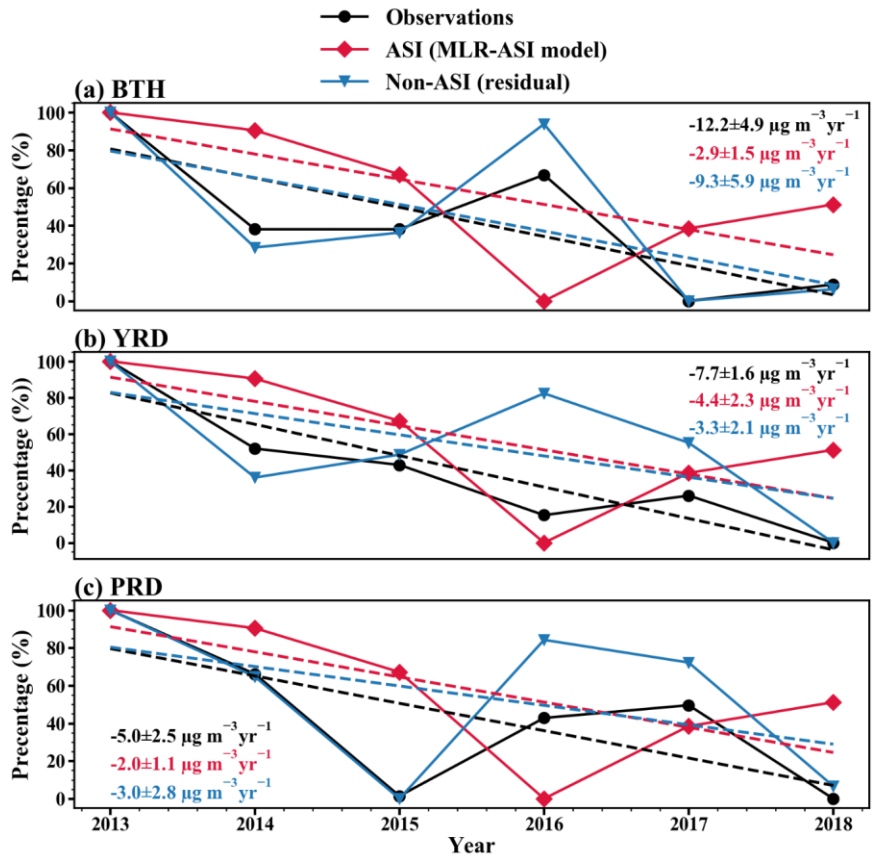

Figure 3: Same as Figure 2 except for MLR-ASI analysis.

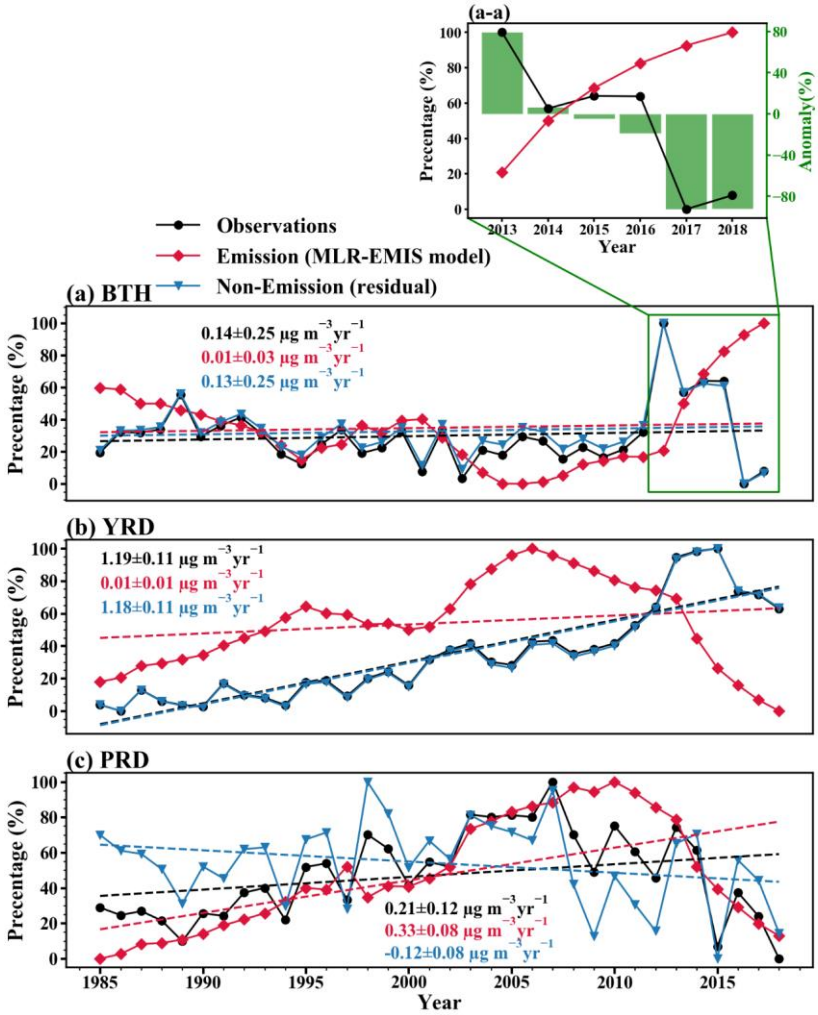

Figure 4: The same as Figure 2 except for time period of 1985–2018. Subfigures 4(a-a) are enlarged schematic representations of the period 2013–2018 in Figure 4(a).

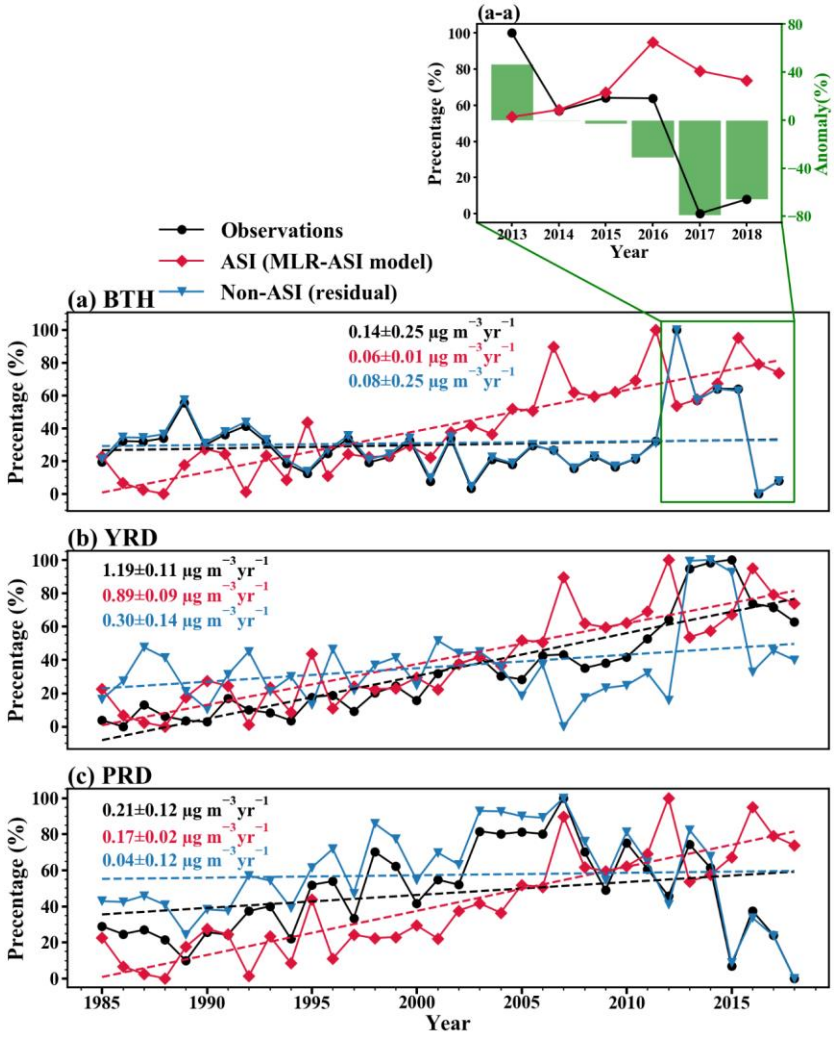

Figure 5: The same as Figure 4 except for MLR-ASI analysis.